

## Multi-Source Snow Cover Monitoring in Eastern Switzerland

Jens Piesbergen, Francesco Holecz, and Harold Haefner Remote Sensing Laboratories, Department of Geography, University of Zurich Winterthurerstrasse 190, CH-8057 Zurich - Switzerland

{piesi, franci, haefner}@geo.unizh.ch

<http://www.geo.unizh.ch/~piesi>

### Abstract

**Methods for the application of ERS-1 SAR and L-5 TM imagery to monitor and map the snow cover in high mountain areas are presented. There are based on geometric and radiometric corrections to calibrate the data. Using the optimal resolution approach ORA synthetic SAR images are calculated to significantly improve the thematic information content. The multitemporal optimal resolution approach MORA uses a sequence of ascending and descending scenes. It builds on the functionality of ORA by coregistering image pairs and extracting geocophysical parameters through successive ratioing of the backscatter information. Wet snow cover monitoring was done by calculating ratios between the backscattering coefficients of the synthetic SAR images and two reference scenes. The climbing of the snow-line could clearly be detected. The potentials and limitations of the approach are discussed. Furthermore snow cover maps based on L-5 TM imagery are discussed.**

*Keywords: snow cover mapping and monitoring, ERS PRI imagery, Landsat TM, multitemporal optimal resolution approach, geometric and radiometric rectification*

### Introduction

Snow cover variations significantly influence the hydrological circulation. Remote sensing data and related techniques offer the opportunity to continuously monitor the snow cover over large areas. Results of snow cover mapping and water equivalent estimation showed the usefulness of electro-optical (EO) data over large alpine basins [1]. However, the use of optical satellite sensors can lead to lack of information, due to bad weather conditions. To overcome this problem interpolations to bridge the missing link between consecutive satellite images are required.

Another possibility is to rely on radar sensors. In terrain with pronounced relief variations, radar backscatter becomes strongly distorted, exhibiting changes in local mean intensity. Furthermore, layover and radar shadow effects produce signals without interpretable thematic information.

It becomes necessary to use the optimal resolution approach ORA to combine SAR data of crossing orbits for each acquisition day [2]. This method produces synthetic images to reduce the layover areas and improve the local mean resolution. Furthermore these images are more easily interpretable than the originals in the initial SAR geometry.

The purpose of this poster is to present the multitemporal optimal resolution approach MORA. It is an extension of ORA. The result of applying MORA to six ascending and descending ERS-1 SAR image pairs over Eastern Switzerland, allows the monitoring of snow coverage from January to July 1993. In addition we evaluate the use of ERS-1 SAR magnitude imagery for change detection in high alpine regions and for snow cover mapping covering large alpine basins and present first results of deriving snow cover maps from electro-optical imagery (EO).

This work consists of three thematic parts, namely the postprocessing of the SAR data including the application of ORA, the monitoring of the snow cover applying the multitemporal aspect of the analysis, and the derivation of snow cover maps based on EO data. Results show that the monitoring of wet snow cover is practicable. Several limitations will be discussed. First results of EO derived maps are presented.

### Datasets

For this study 12 ERS-1 SAR PRI scenes covering a part of Eastern Switzerland (1260km<sup>2</sup>, Figure 1) acquired in a 35-day repeat orbit cycle between January 1993 and July 1993 from ascending and descending orbits were used. The satellite overflight of the ascending swath (21:30 UTC) and the descending swath (10:10 UTC) took place on the same date (Figure 2). Two Landsat-5 Thematic Mapper (TM) scenes dated 15.02.93 and 22.05.93 (09:10 UTC) are also available (Figure 3).

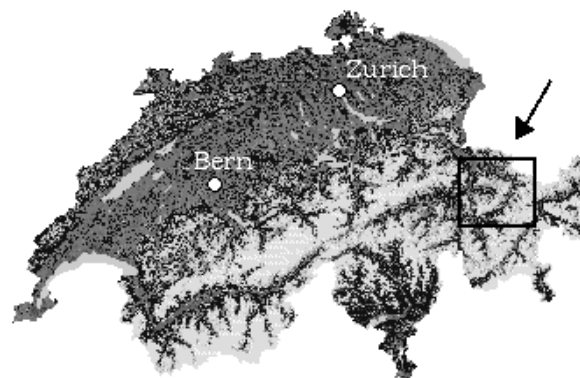


Figure 1: Location of testsite in Eastern Switzerland

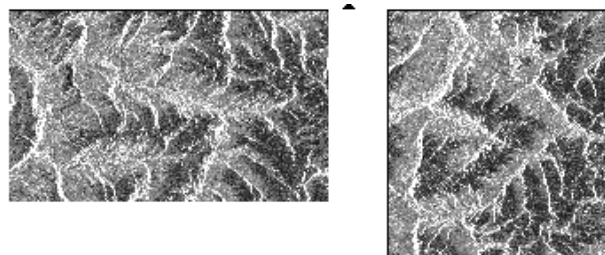


Figure 2: Subset of ERS-1 PRI imagery 01.05.93, descending orbit (left), ascending orbit (right)

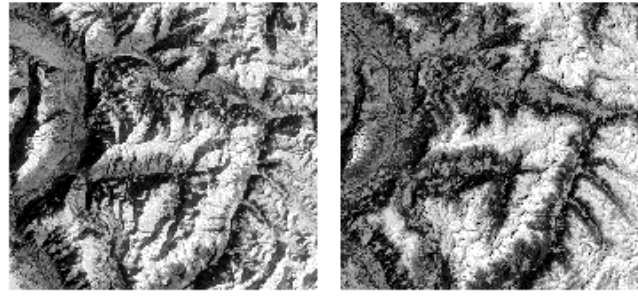


Figure 3: Subset of TM imagery (nir) covering northern part of Grisons; 15.02.93 (left) and 22.05.95 (right)

For this project a digital elevation model (DHM25) with a grid size of 25m and a height resolution of 0.1m is available [3]. It covers 6 sheets of Swiss Topographic map 1:25'000.

Meteorological data (air temperature, cloud coverage, precipitation, wind velocity) and snow parameters (snow temperature, snow depth, density, grain size and type, snow surface type, and the load-bearing capacity) were collected during the field measurements on the January, February and March overflights.

## Method

Figure 4 explains the various steps of MORA. It is based on the ORA which allows the radiometric calibration of the SAR data in the initial original geometry (slant range or ground range representation), as well as the combination of ascending and descending orbit imagery in a cartographic reference system using the highest local ground resolution. Layover areas are dramatically reduced and the extraction of thematic information is significantly improved. Prerequisites are a DEM and a precise terrain geocoding. MORA uses a sequence of ascending and descending SAR image pairs. It builds on the functionality of ORA coregistering image pairs and extracting of geocophysical parameters through successive ratioing of the image information.

After the speckle reduction and the selection of a reference scene pair for the geocoding process, first an image coregistration is done using a quadratic transformation function and a nearest neighbour resampling by setting several tie points in a reference scene and the slave scenes. This step is performed to produce a uniform image illumination geometry. Subsequently, the geocoding procedure has to be done for a single ascending and descending image geometry. Second, the removal of relief induced radiometric distortions requires a highly precise geocoding of the image information. This geometric correction must consider the sensor and the processor characteristics, and is therefore based on a rigorous range-Doppler approach [4].

Radiometric distortions caused by the relief are removed using value added products such as local incidence angle and local resolution maps. These products are calculated directly from the DEM by reconstructing the original illumination geometry for each individual backscatter element. This information is transformed into the initial SAR geometry (PRI: ground range geometry) and used to derive the backscattering coefficient  $\sigma_0$  and  $\gamma$  [5]. To avoid geometric and radiometric distortions of the radar signal  $\gamma$  is calculated in the original SAR geometry, for the reference scene pair only. The radiometric correction also include an antenna gain pattern correction (AGP). In [6] it is shown, that in the ERS-1 case, topographic effects do not significantly affect the AGP correction. It was therefore not taken into account.

The crossing images can now be combined to produce a synthetic product containing improved thematic information. To avoid radiometric changes and to minimize geometric distortions, a nearest neighbour method with a pixel spacing of 25 m was applied. The new synthetic image is obtained from the two geocoded images by applying ORA. For the synthetic image the normalized radar backscattering coefficient  $\gamma$  is taken from the orbit with the better local ground resolution.

Wet snow cover mapping is done by calculating the ratio between the backscattering coefficient values of the synthetic SAR images and that of a snow-free reference scene as proposed in [7]. The ratio of the backscattering coefficients corresponds to the difference between the  $\gamma$ -values expressed in dB. For each synthetic scene the ratio to a reference scene is calculated. As reference, a snow-free summer or an early autumn scene as well as a scene covered by dry snow can be chosen. Together with the analysis of the field measurements and a the interpretation of the TM scenes the extracted thematic feature is a sequence of wet snow coverage.

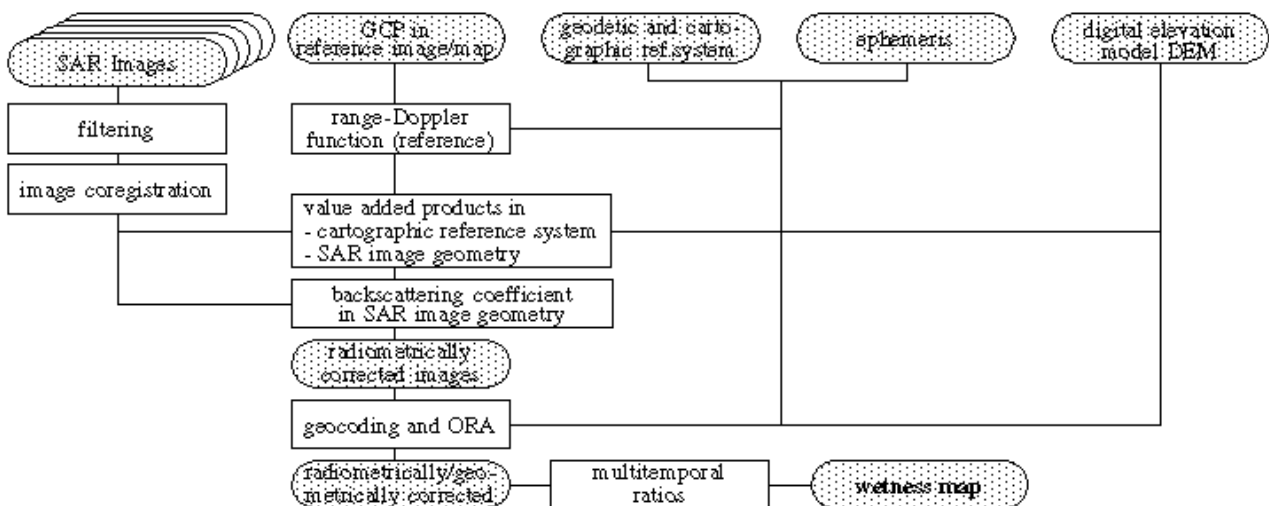


Figure 4: Postprocessing steps for SAR data with the multitemporal optimal resolution approach MORA

Figure 5 shows the various steps of the processing of the TM imagery. The system corrected images have undergone several geometric transformations. Because of a nearest neighbour resampling procedure during the image generation nearly every 70th row is duplicated in order to reach the nominal TM resolution of 30m. These double rows cause unwanted effects along edges and linear elements, e.g. roads. By means of similarity detection algorithm the double rows have been determined and eliminated afterwards. Satellite images are affected with a parallax due to terrain height variations. The apparent displacement can amount to several pixels [8]. The applied geocoding algorithm consists of an affine transformation taking into account the relief displacement by using a DEM. To correct direct, indirect and diffuse illumination and atmospheric effects a physically-based model proposed by [9] is used. The estimation of surface reflectance is done in a two-step procedure. First irradiance components and atmospheric parameters are calculated for horizontal surface using 6S (atmo-module), then the influence of the topography is integrated using DEM data (topo-module).

Using the geometrically and radiometrically calibrated data thematic interpretation in respect to an accurate snow cover classification is based on a robust ratio model. Dividing the calibrated reflectance value of the near-infrared channel with the respective pixel value of the green channel results in an accurate snow cover distribution map.

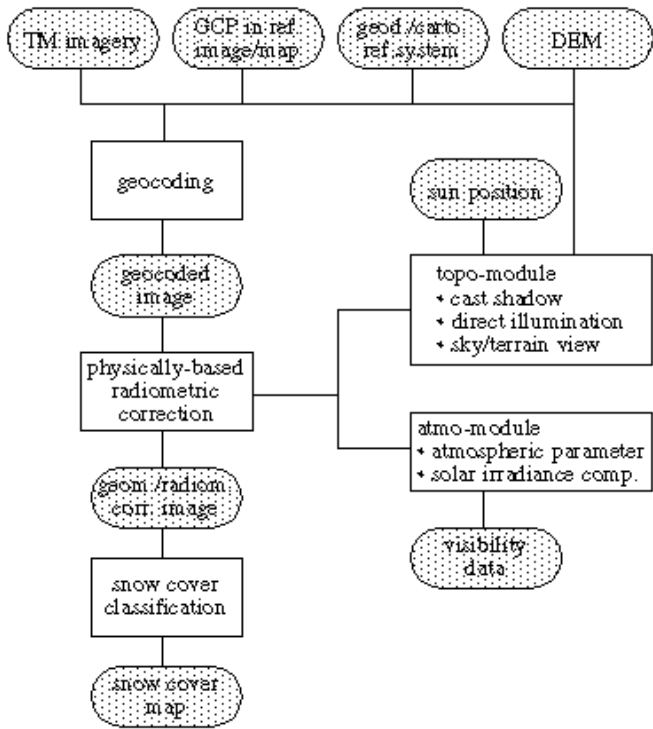


Figure 5: Data processing of TM imagery

### Results

The residuals for the SAR image coregistration are approximatively 0.5 pixels in azimuth and 0.6 pixels in range for the ascending scenes and 0.9 and 0.7 pixels for the descending scenes, respectively. The reconstruction of the original illumination geometry using the range-Doppler function was done with the SAR image pair dated 01.05.93 because the orbit information had the best time resolution (4sec). It produced residuals of about 1.1 pixels in range direction and around 4 Hz in azimuth for the ascending case and 0.9 pixels in range and 6.5 Hz for the descending scene, respectively.

Figure 6 shows SAR layover masks in the Swiss Reference System for the date 01.05.93. 26% (desc.) and 38% (asc.) of the available data are covered by layover. These areas are not thematically interpretable. Applying ORA reduces these useless information dramatically to 5% (Figure 7).

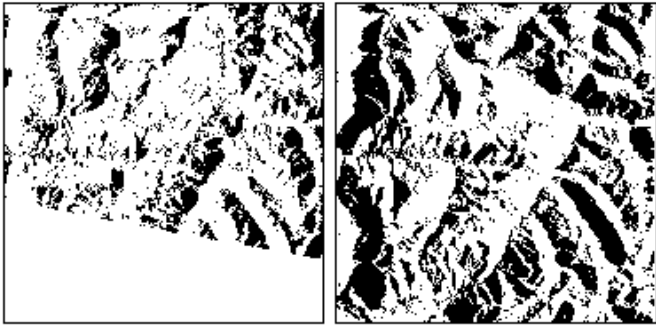


Figure 6: Layover areas in descending, 26%, (left) and ascending, 38%, (right) orbital imagery

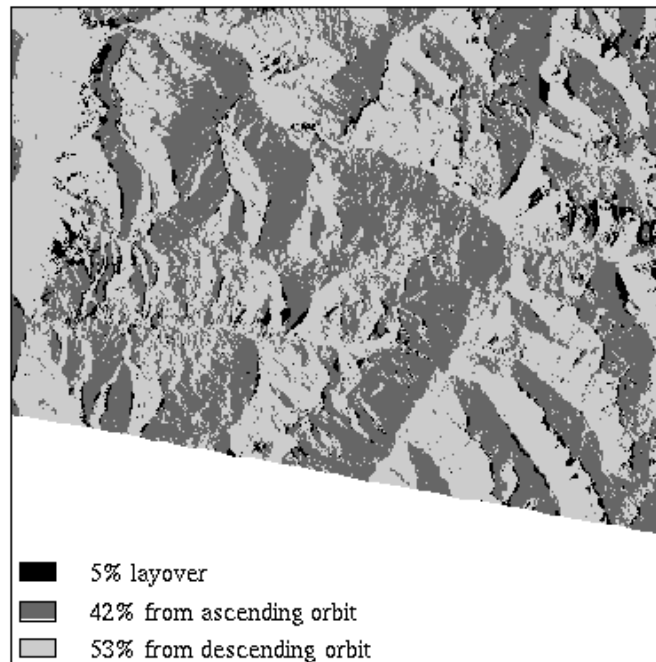


Figure 7: ORA origin map from which SAR scene information is taken to compose a synthetic SAR image

Due to the orbit geometry and the given topography 53% of the synthetic image pixels originate from descending orbit imagery, while 42% are taken from the ascending orbit. Over 48% of the testsite backscatter coefficients are available from both orbits. The resulting smaller number by calculating the local ground resolution of these elements indicate the chosen image source. For these data the origin of the gamma-values are equal distributed (24%, Figure 8 left). Figure 8 (right) shows the local ground resolution for this alpine region. Most of the SAR pixels represent 30-45m2.

As reference dates for the thematic interpretation the acquisition dates 16.01.93 and 10.07.93 were chosen because the first had relatively dry snow conditions and in the latter most parts of the scene were snow free except some areas near ridges with permanent snow coverage. In spite of the different times of day of the SAR data acquisitions for one image pair the backscattering coefficient gamma did not change significantly. The reason is, that 1) due to the stable air temperature conditions no snow melting process had started (20.02.93) and 2) for the 27.03.93 scene the already started melting process during the day (early spring at this sea level) causes a relative wet snow layer which could not have refrozen before the ascending overflight. The load-bearing capacity of the snow surface was a depth of a ski track while the surface roughness was wavy to light furrowed. For the 01.05.93 and 05.06.93 scenes the snow showed typical spring properties: wet, partly melted, coarse grain size, low hardness.

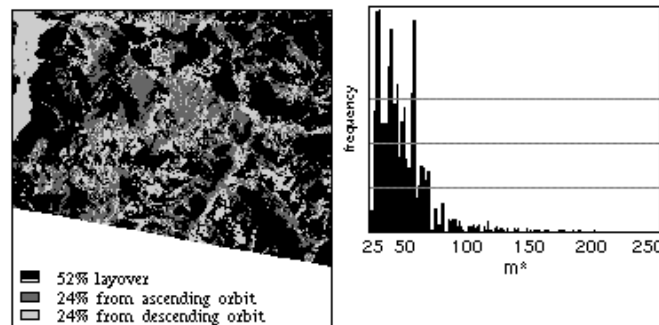


Figure 8: ORA decision map (left) and distribution of local ground resolution (right)

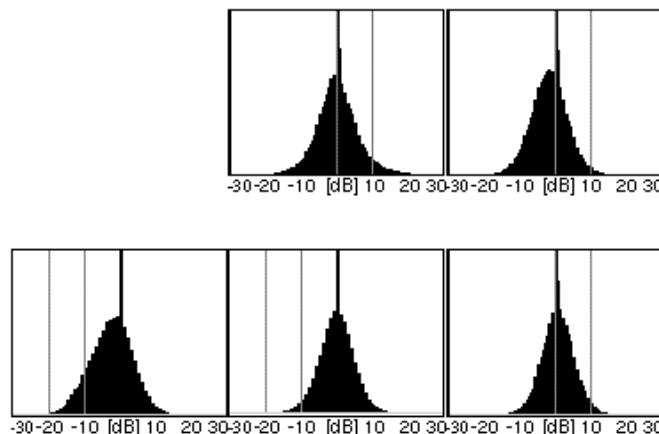


Figure 9: Distribution of ratio values compared to 16.01.93

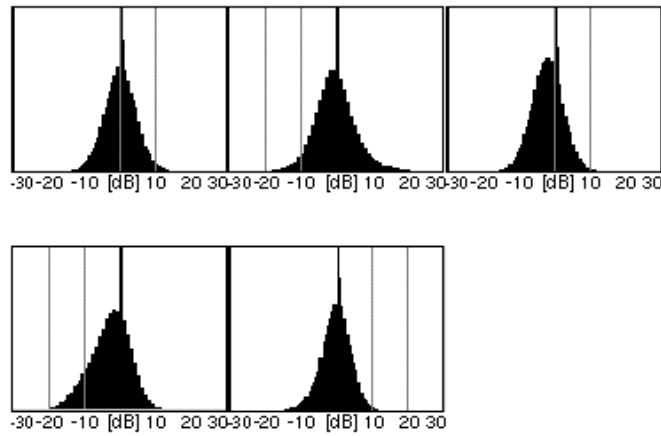


Figure 10: Distribution of ratio values compared to 10.07.93

Figure 9 and Figure 10 show the calculated ratio values for the snow coverage from January until July compared to the reference scenes 16.01.93 and 10.07.93 respectively. The resulting histograms show significant differences. The increase of the wetness can be identified with a left-sided skewness of the histograms. The snowfree July is skewed to the right.

The multitemporal dataset printed in Figure 13 are sequences of "wet snow coverage". The grayscale values indicate the increase of wetness and ranges from -0.5dB to -12dB and was applied to guarantee comparable results to [10]. The extent of the snow coverage is strongly correlated to the topography during the melting season, especially seen in May and June. January and February are relatively dry. Within the March scene an increase of the wetness conditions can be notified. Between the May and the June date the snow-line moved to higher altitudes. July is snowfree but the remaining wetness indicate wet soil conditions.

Figure 11 illustrates the different sun illumination conditions during the TM data acquisition time over the test site. Strong cast shadow areas can be clearly identified. Coarse snow cover maps are presented in Figure 12 for the 15.02.93 and 22.05.93 dates. Black indicate the snow coverage. It is strongly correlated to the topography. But some misclassifications in lower parts of the valleys have to be mentioned. Due to saturation effects the snow cover mapping procedure was not applied to the completely radiometrically corrected TM data. But comparing these maps with those of Figure 13 the results are promising. Further investigations have to be carried out.

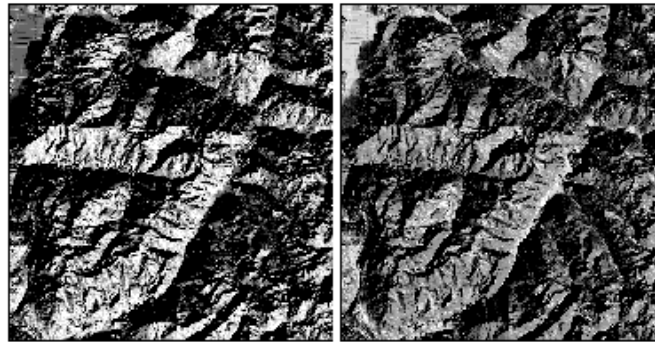


Figure 11: Illumination conditions during TM data acquisition 09.30 UTC on 15.02.93 (left) and 22.05.93 (right).  
Digital terrain model (DHM25): © Swiss Federal Office of Topography (1524a)

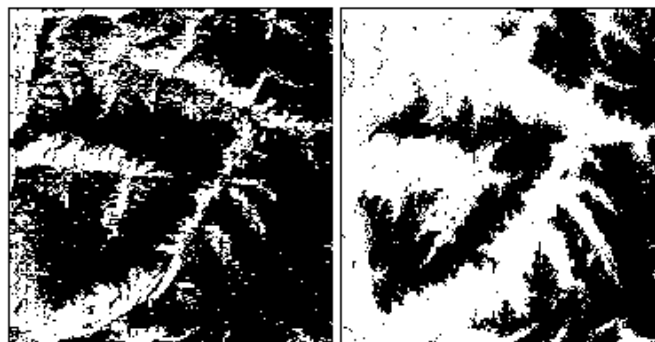


Figure 12: Snow cover maps based on TM imagery, 15.02.93 (left) and 22.05.93 (right)



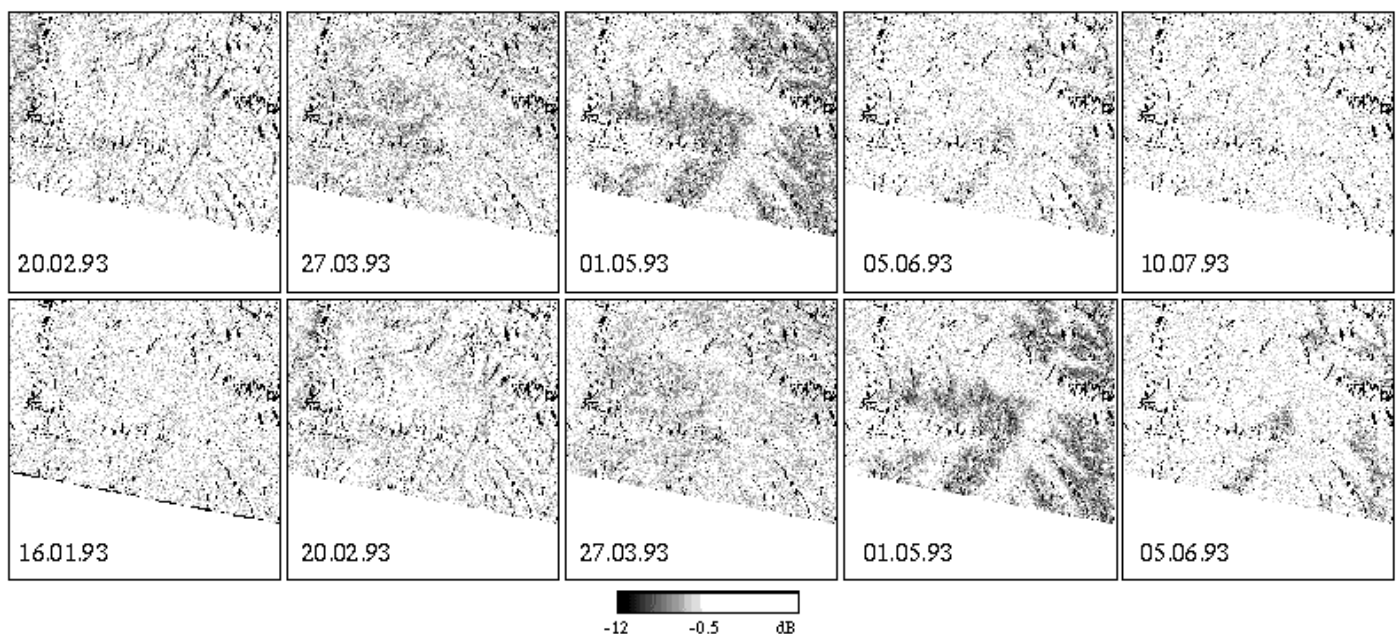


Figure 13: Sequences of wet snow coverage: ratio values relative to 16.01.93 and 10.07.93

## Discussion and conclusions

Following achievements and limitations have to be mentioned and taken into account.

The optimal resolution approach ORA increases the availability of thematic SAR imagery in mountainous regions dramatically.

ORA can also be performed over large areas (1260km<sup>2</sup>).

The multitemporal optimal resolution approach MORA is a practicable method for change detection using ERS magnitude data.

A dry-snow or snow-free reference scene for calculating the ratio results in qualitatively comparable results.

Taking into account several reference scenes considerably extend the dataset sequence.

Snow/no-snow maps based on SAR PRI data cannot directly be calculated. Nevertheless, a coarse discrimination of wet snow can only be made in wide open areas and together with additional information, i.e. meteorological data and specific thematic parameters.

Between snow-covered and snow-free zones, a few areas are erroneously interpreted as snow-covered. This confusion may be caused by the existing wet soil conditions.

Vegetation changes have also to be considered.

Due to the coregistration procedure the geometric accuracy is less than that achievable in geocoding scene by scene. An advantage of the coregistration process is that for all scenes an information pixel is always retrieved from the same orbit.

The low local spatial ground resolution in sloped areas limits the accuracy of the thematic interpretation.

The geocoding procedure for L-5 TM data consisting of an affine transformation taking into account the relief displacement results in a high accurate product.)

The physically-based radiometric correction is strongly limited to the scene specific contents. Snow reflectance values saturate strongly. More investigations are required and will be carried out.

Due to saturated image information only a coarse snow cover classification could be achieved.

Methods for mapping and monitoring wet snow cover in alpine terrain were presented. Analyzing advantages and disadvantages of the use of EO or SAR sensors, in general it can be concluded that EO data are more suitable for snow cover mapping purposes. On the other hand SAR systems are absolute necessary to retrieve certain snow parameters and to monitor the melting process. However, there is still a great unrealised potential in analysing multitemporal and multisource data for geoecological applications.

## Acknowledgments

This work has been supported by the [Swiss Academy of Science](#) (Project 20-41889.94). The ERS-1 SAR data were made available for AO.CH2 experiment by the [European Space Agency](#) ESA. Landsat-5 Thematic Mapper data provided by [Eurimage](#). Digital terrain model (DHM25): © [Swiss Federal Office of Topography](#) (1524a).

## References

- Seidel, K., Ehrler, C., Martinec, J., Turpin, O., 1997:  
Derivation of statistical snowline from high resolution snow cover mapping. *Proceedings of EARSeL Workshop "Remote Sensing of Land Ice and Snow"*, Freiburg, Germany, 17-18 April 1997.
- Haefner, H., Holecz, F., Meier, E., Nüesch, D., and Piesbergen, J., 1993:  
Capabilities and Limitations of ERS-1 SAR Data for Snowcover Determination in Mountainous Regions. *Proc. Second ERS-1 Symposium*, Hamburg, pp. 971-976.
- Swiss Federal Office of Topography, 1996:  
Das digitale Höhenmodell des Bundesamtes für Landestopographie. Wabern, Switzerland.
- Meier, E., Frei, U., and Nüesch, D., 1993:  
Precise Terrain Corrected Geocoded Images. Chapter 7 in: *SAR-Geocoding - Data and Systems*, Wichmann-Verlag, edited by Schreier, G., pp. 173-185.
- Holecz, F., Meier, E., Piesbergen, J., Nüesch, D., and Moreira, J., 1994:  
Rigorous Derivation of Backscattering Coefficient. *IEEE Geoscience and Remote Sensing Newsletter*, **Nr. 92**, pp. 6-14.
- Holecz, F., Freeman, A., and van Zyl, J., 1995:  
Topographic Effects on the Antenna Gain Pattern Correction. *Proceedings of IGARSS'95*, Florence, Italy.
- Rott, H., and Nagler, T., 1993:  
Capabilities of ERS-1 SAR for Snow and Glacier Monitoring in Alpine Areas. *Proc. Second ERS-1 Symposium*, Hamburg, pp. 965-970.
- Frei, U., 1993:  
Compilation of cartographic and spaceborne remote sensing data for thematic/topographic mapping. *Remote Sensing Series*, **Vol. 22**, Dept. of Geography, University of Zurich, Zurich.
- Sandmeier, S., 1996:  
A physically-based radiometric correction model. *Remote Sensing Series*, **Vol. 26**, Dept. of Geography, University of Zurich, Zurich.
- Piesbergen, J., Holecz, F., Haefner, H., 1995:  
Snow cover monitoring using multitemporal ERS-1 SAR data. *Proceedings of IGARSS'95*, Florence, Italy, pp. 1750-1752.

